1

Background and techniques

The idea behind spintronics, to employ spins in *non-magnetic materials* (NM) for information storage and processing, is ambitious. The spin degree of freedom of an electron possesses only a short lifetime due to interactions with the host material. This results for NM generally in an equilibrium state without a dominant spin orientation. Thus, current research focuses on the exploration of possibilities to create non-equilibrium spin accumulations with long lifetimes, to transport and manipulate them. There are several techniques which employ different effects to create a non-equilibrium spin distribution in a NM. Spin polarizations created by optical excitation or electrically injection from a *ferromagnet* (FM) are the most common techniques, but also the so-called *spin Hall effect* (SHE), using different scattering directions of the spins, can also be employed to create spin accumulations within a material [15, 32, 33].

A non-equilibrium spin polarization can be created optically by illuminating a material with circular polarized light [10]. The angular momentum of the light is transferred into the spin momentum of the electrons, also known as *optical orientation.* This process is highly efficient for direct band gap materials, such as III-V *semiconductors* (SC), but it has also been demonstrated in Si with a spin polarization of a few percent [10]. This is mainly due to the short spin relaxation time compared to the recombination time of the spins. By engineering a *light emitting diode* (LED)

band structure, this effect can be reversed to measure spin accumulations by detecting the circular polarization of the light emitted by this so-called *spin-LED* [11]. Similarly, a spin-laser band structure has been recently engineered to intrinsically pump spin polarized electrons and generate coherent polarized light [34].

A simpler and more viable way for applications is the injection of spins electrically from a spin polarized source. Ferromagnets have been established as such sources, since they exhibit an intrinsic spin polarization in thermal equilibrium. A current from a FM into a NM is consequently spin polarized and creates a non-equilibrium spin accumulation in the NM. The electric potential probed by a FM contact is also spin dependent. This means that FMs can be used in an all-electrical setup to create and detect spin polarizations in NM. That is advantageous, since it is simple to fabricate, to control and better aligned with possible future integration into logic devices.

Initially such contacts were not easy to realize, since the *conductivity mismatch* between the FM and the NM yields a low efficiency of the spin transfer. This motivated the idea of introducing a *tunnel barrier* (TB) [35]. Using FM tunnel contacts lead to several breakthrough achieving large spin accumulations in NM materials, including in graphene [36] and silicon [18] at room temperature, which encourages developments for applications for everyday technology. Since then, a race to optimize fabrication techniques and study new materials started. Not only different substrates are investigated, but also FM and TBs, since they can affect the spin accumulation inside the substrate significantly.

Here we discuss the basic idea of spin injection and detection with a FM. Consequently, its drawbacks and experimental solutions are presented. Finally, we present the recent advances made in different materials, such as Si, graphene, *hexagonal boron nitride* (h-BN), *transition metal dichalcogenides* (TMDC) and *topological insulators* (TI).

1.1 Ferromagnetism and spin polarization

Magnetism in general stems from the unpaired spins of the electrons. In FM transition metals, such as iron, cobalt and nickel, the 3d orbital is not fully occupied, so electrons can arrange freely according to the *Hund's rules* and the *Pauli principle* to achieve the configuration with the lowest energy. The energy difference between parallel (triplet) and anti-parallel (singlet) spin configuration is the so-called exchange energy. If the gain in exchange

energy of a parallel spin alignment is larger than the increase in kinetic energy, the material exhibits a finite magnetization in thermal equilibrium and is called a FM. This results in a splitting of the *density of state*s (DOS) at the Fermi level, which means the available states N for up-spins is larger than for down-spins[1]: $N_\uparrow > N_\downarrow$. This can be used to define the intrinsic spin polarization in the FM as

$$P = \frac{N_\uparrow - N_\downarrow}{N_\uparrow + N_\downarrow}. \tag{1.1}$$

More interesting is the spin polarization of an electron current. In 1936, Mott proposed that a charge current is made of two independent spin currents [4, 5]. He realized that FMs exhibit a spin dependent scattering when magnon scattering is suppressed. Consequently, the conductivity σ can be expressed as the sum of two independent, but spin dependent conductivities $\sigma_\uparrow$ and $\sigma_\downarrow$: $\sigma = \sigma_\uparrow + \sigma_\downarrow$. This is known as the two-current model and has since been further developed [37, 38]. These spin dependent conductivities can be expressed in the Einstein equation as

$$\sigma_{\uparrow\downarrow} = N_{\uparrow\downarrow} e^2 D_{\uparrow\downarrow}, \text{ with } D_{\uparrow\downarrow} = \frac{1}{3} v_{F\uparrow\downarrow} l_{e\uparrow\downarrow}, \tag{1.2}$$

where e is the electron charge and $D_{\uparrow\downarrow}$ is the spin dependent diffusion constant, expressed as a function of the Fermi velocity $v_{F\uparrow\downarrow}$ and the mean free path of the electron $l_{e\uparrow\downarrow}$. Ferromagnets, FM insulators and their interfaces show this spin dependent conductivity, where the polarization of the current can be written as

$$P = \frac{\sigma_\uparrow - \sigma_\downarrow}{\sigma_\uparrow + \sigma_\downarrow} \tag{1.3}$$

and is experimentally obtained for Fe (45%), Co (42%), Ni (27%) [39] as well as some tunnel interfaces [28]. In the literature, P is often referred to as β or γ to distinct between the bulk and the interface polarization, respectively.

For interfaces between a FM and a NM the spin dependent conductance can be defined as $G_{\uparrow\downarrow} = \left(R^I_{\uparrow\downarrow}\right)^{-1}$, where $R^I_{\uparrow\downarrow}$ is the spin dependent resistivity of the barrier.

Equation (1.3) can also be directly used to describe the resistance switching in *magnetic tunnel junctions* (MTJ). In a MTJ two FMs are separated by a thin insulating barrier. Altering the magnetization configuration between

[1] We define the up-spins in general as majority spins.

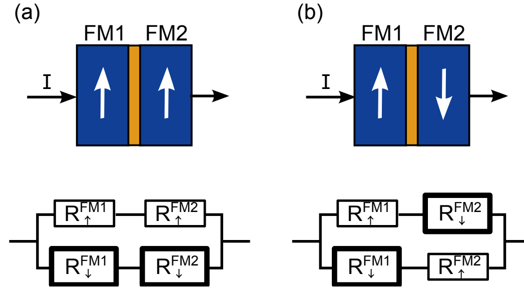

Figure 1.1: Schematic and resistor model of a ferromagnet (FM)/tunnel barrier (TB)/FM structure with (a) parallel magnetization orientation and (b) anti-parallel magnetization orientation. The FM resistance for up-spins is lower than the resistance for down-spins.

the FMs (either parallel or anti-parallel) results in a change in the measured resistance across this heterostructure (Figure 1.1). Assuming the spin is preserved while tunnelling, the *tunnel magnetoresistance* (TMR) can be extracted:

$$TMR = \frac{G_p - G_{ap}}{G_p + G_{ap}} = \frac{2\gamma_1\gamma_2}{1 - \gamma_1\gamma_2}, \tag{1.4}$$

where G_p and G_{ap} is the conductivity through the FM layers for parallel and anti-parallel magnetization orientation, respectively. The right hand side of Equation (1.4) can be derived using Equation (1.3) in the different resistance configurations, whereas γ_1 and γ_2 are the interface polarizations of FM1 and FM2, respectively. These polarizations were historically believed to be the intrinsic FM polarization defined by the DOS [40], but experiments demonstrated that the polarization is very sensitive to the used interface material, its transparency, roughness and contamination, especially within the first few atomic layers of the interface [7]. Also the crystal structure and lattice matching of both FM and insulator seem to have a significant influence. Therefore, MTJ structures are nowadays used to characterize interfaces and barrier materials. This interface dependency is also relevant for transparent and tunnelling junctions on NM, which will be discussed in the next sections.

1.2 Spin scattering mechanisms

Spins in any material exhibits only a finite lifetime due to SO and *hyperfine* (HF) interactions. This spin lifetime τ, together with the spin diffusion constant D, are important parameters in spintronics, since they define the

possible distance a spin can be transported:

$$\lambda = \sqrt{D\tau}. \tag{1.5}$$

Two main mechanism contribute to the spin relaxation due to SO interactions: *Elliott-Yafet* (EY) and *D'yakonov-Perel* (DP) [1].

The EY mechanism describes a coupling between the up- and down-spin state due to lattice symmetry in presence of scattering centres, such as phonons, boundaries or impurities. That means a scattering electron has a finite probability to flip its spin state. The spin flip probability increases with the scattering probability, which scales also with the atomic mass and size of the atoms. This was first discussed for elemental metals, but applies also for most pure crystals to a certain degree and its strength depends mainly on the mass of the constituent atoms. Silicon and graphene have a low atomic mass and hence exhibit a low SO coupling due to EY, which should result in long spin lifetimes. In contrast, TIs, such as Bi_2Se_3, have a strong SO interaction, which gives rise to their atypical band structure (see Section 1.6.5).

D'yakonov-Perel describes a mechanism in systems without inversion symmetry. The presence of two distinct atoms in the Bravais lattice leads to bulk inversion asymmetry (*Rashba-Dresselhaussen*). A built-in or external electric field yields structural inversion asymmetry (*Bychkov-Rashba*). Both types result in an *electrostatic potential gradient* $\vec{E}$. Spins moving with a velocity $\vec{v}$ (relative to the speed of light c) through this electric field are affected by an effective *magnetic field* $\vec{B} = \frac{\vec{v}}{c} \times \vec{E}$. If the coupling is strong enough, this translation can be employed to manipulate the spins within the material by using an external electric field (also called *Rashba effect*). Transition metal dichalcogenides have a large atomic mass and exhibit no inversion symmetry resulting in a strong SO interaction due to EY and DP. Despite the enhanced spin scattering, a valley splitting occurs, which are occupied by different spin states and highly interesting for spintronic applications (see Section 1.6.3).

The HF interaction is a coupling of the magnetic moments of the electrons and the nuclei. This interaction dominates for localized electrons, for example in quantum wells or quantum dots. It is negligible if the magnetic moment of the nuclei is zero, which occurs for systems with a full nuclear shell, for example silicon (^{28}Si) and graphene (^{12}C). Inducing HF interaction in graphene can be achieved by artificially growing it with an isotope with a remaining nuclear spin, for example ^{13}C [41]. Alternatively, the material *black phosphorous* (BP), whereof a 2D layer is called phosphorene,

has similar properties as TMDCs, but a natural nuclear spin resulting in a strong HF coupling.

In practice, crystals are not ideal, intentionally or unintentionally doped, contain impurities, adatoms, lattice errors and ripples for 2D materials, which can induce scattering centres and have to be considered as possible factors reducing the spin lifetime.

1.3 Spin injection and accumulation

In a NM the conductivities for up- and down-spins are identical. That means that an applied current through a FM/NM junction experiences a discontinuity in the spin dependent conductivity. This yields to the creation of a spin accumulation at the interface and hence a splitting of the chemical potential for both kinds of spins, $\mu_\uparrow$ and $\mu_\downarrow$. A general definition for the electrochemical potential is

$$\mu = \frac{n}{N}, \tag{1.6}$$

where N is the available states at the Fermi level and n is the excess particle density. The spin accumulation decays exponentially within the FM and the NM with a respective penetration depth λ_{FM} and λ_{NM} (see Figure 1.2). The spin dependent current density $j_{\uparrow\downarrow}$ can be expressed by[2]

$$j_{\uparrow\downarrow} = \frac{\sigma_{\uparrow\downarrow}}{e}\partial_x \mu_{\uparrow\downarrow}. \tag{1.7}$$

This current can gradually change when spin flip processes are considered. Introducing the spin flip times $\tau_{\uparrow\downarrow}$ for an up to down spin-flip and $\tau_{\downarrow\uparrow}$ for the revered process leads to the expression

$$\frac{1}{e}\partial_x j_{\uparrow\downarrow} = \mp\frac{n_\uparrow}{\tau_{\uparrow\downarrow}} \pm \frac{n_\downarrow}{\tau_{\downarrow\uparrow}}. \tag{1.8}$$

In thermal equilibrium no net spin scattering should take place and

$$\frac{N_\uparrow}{\tau_{\uparrow\downarrow}} = \frac{N_\downarrow}{\tau_{\downarrow\uparrow}}. \tag{1.9}$$

A diffusion equation, describing the complete spin flip process, can be obtained by combining Equations (1.2) and (1.9):

$$\partial_x^2 \left(\mu_\uparrow - \mu_\downarrow\right) = \frac{\left(\mu_\uparrow - \mu_\downarrow\right)}{D \cdot \tau}, \tag{1.10}$$

[2] We assume a simplified one-dimensional (1D) channel along the current direction. Equally, this model can be extended into three dimensions.

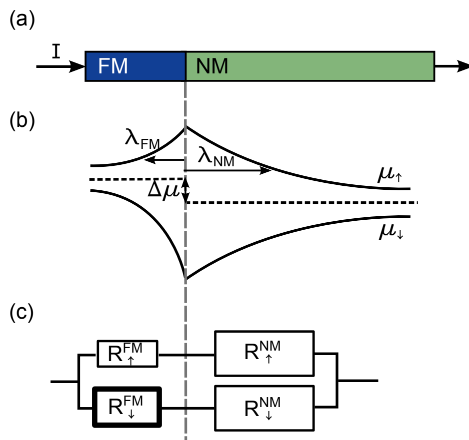

Figure 1.2: Spin current through a FM/NM interface. (a) Schematic of a FM/NM junction. (b) Chemical potentials for up- and down-spins at the barrier-free interface. A splitting $\Delta\mu$ between the equilibrium potentials occurs due to the spin dependent conductivities in the FM. The spin diffusion length is usually much shorter for FM than for NM. The potential drop due to the applied current is neglected in this diagram. (c) Equivalent resistor network for this junction. The spin dependent resistances in the FM are small compared to the NM.

where the spin lifetime is defined as $\tau = \left(\tau_{\uparrow\downarrow}^{-1} + \tau_{\downarrow\uparrow}^{-1}\right)^{-1}$ and the average spin diffusion constant can be written as $D = \frac{D_\uparrow D_\downarrow (N_\uparrow + N_\downarrow)}{N_\uparrow D_\uparrow + N_\downarrow D_\downarrow}$. Equation (1.10) can generally be solved as

$$\mu_\uparrow - \mu_\downarrow = \tilde{a} \cdot \exp\left(-\frac{x}{\lambda}\right) + \tilde{b} \cdot \exp\left(\frac{x}{\lambda}\right), \tag{1.11}$$

where λ comes from Equation (1.5), and $\tilde{a}$ and $\tilde{b}$ are integration constants. Using the ansatz where the charge current is conserved, that means $\partial_x j = \partial_x (j_\uparrow + j_\downarrow) = 0$, and Equation (1.7), the chemical potential for both spins can be separately derived as

$$\mu_{\uparrow\downarrow} = a + b \cdot x \pm \frac{c}{\sigma_{\uparrow\downarrow}} \exp\left(-\frac{x}{\lambda}\right) \pm \frac{d}{\sigma_{\uparrow\downarrow}} \exp\left(\frac{x}{\lambda}\right). \tag{1.12}$$

For a FM/NM contact the constants a, b, c and d can be determined assuming that at the interface the spin dependent electrochemical potentials are continuous, the spin currents are conserved, and interface scattering and resistances are neglected [42]. Defining the equilibrium chemical potential

$\mu = P\mu_\uparrow + (1-P)\,\mu_\downarrow$, a potential difference can be derived as

$$\Delta\mu = \mu_{FM} - \mu_{NM} = \frac{\beta^2 \left(\frac{\lambda_{NM}}{\sigma_{NM}}\right)\left(\frac{\lambda_{FM}}{\sigma_{NM}}\right)\cdot eI}{\left(\frac{\lambda_{FM}}{\sigma_{NM}}\right) + (1-\beta^2)\left(\frac{\lambda_{NM}}{\sigma_{NM}}\right)}, \tag{1.13}$$

where β is the intrinsic spin polarization of the FM defined in (1.1), and λ and σ describe the spin diffusion length and total conductivity, respectively, in either the FM or NM. Dividing Equation (1.13) by eI a spin coupled interface resistance R_I arises (see Figure 1.2b). That is remarkable, since we neglected any other interface resistances and stems simply from the discontinuity of the conductivities across the barrier. Furthermore, Equations (1.12) and (1.13) define the spin splitting $2\mu_0$, which is at its maximum at the interface:

$$2\mu_0 = \mu_\uparrow - \mu_\downarrow = \frac{2\Delta\mu}{\beta}, \tag{1.14}$$

whereas $\pm\mu_0$ describes directly the chemical potential for up and down spins in the NM, respectively. Equation (1.3) and (1.13) can be used to derive the spin polarization of the current through the interface

$$\gamma = \frac{I_\uparrow - I_\downarrow}{I_\uparrow + I_\downarrow} = \frac{\beta \frac{\lambda_{FM}}{\sigma_{FM}}}{\frac{\lambda_{FM}}{\sigma_{FM}} + (1+\beta^2)\frac{\lambda_{NM}}{\sigma_{NM}}}. \tag{1.15}$$

This shows that the spin coupled interface resistance, the potential splitting and the spin polarization mainly depend on the ratios $\frac{\lambda_{FM}}{\sigma_{NM}}$ and $\frac{\lambda_{NM}}{\sigma_{NM}}$. As discussed earlier, most FM have a small spin diffusion length, $\lambda_{FM} \ll \lambda_{NM}$. Therefore, the denominator in Equation (1.15) becomes much larger than the numerator, hence the current polarization P is reduced. This becomes even more pronounced when injecting into SCs, since they usually exhibit a much lower conductivity than metals. This problem is therefore known as *conductivity mismatch*. Spins injected in the NM have a high tendency to diffuse back into the FM, where they decay faster, due to the high SO coupling and short spin diffusion length. This mismatch can be solved by introducing a TB.

1.4 Spin injection and detection with tunnel contacts

Tunnel barriers play a crucial role for spin injection. Coupled to a FM they provide a high spin dependent resistance and therefore enhance the

magnitude of the spin signal (Figure 1.3). Their high spin dependent resistance circumvents the conductivity mismatch problem and prevents spins, once injected in the NM, to diffuse back into the FM and losing their spin information faster. Therefore, spin injection and detection through a TB shows a much higher efficiency than a direct contact and is well established as reliable source for spin currents [18, 28, 36, 43].

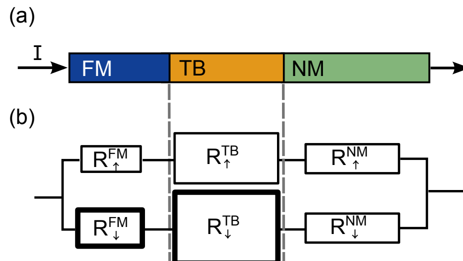

Figure 1.3: Spin current through a FM/TB/NM interface. (a) Schematic of a FM/TB/NM junction with a TB. (b) Equivalent resistor network for this junction. The spin dependent resistances in the TB are large compare to the NM and the FM.

Even though the idea seems simple, there are various configurations in which spin accumulations and transport can be created and measured in different materials. This section describes three common techniques, which were used for the studies discussed in the following chapters.

1.4.1 Local magnetoresistance measurement

Applying a current through two FM tunnel contacts connected by a NM is a simple way to create a non-equilibrium spin accumulation. On one hand, this often called two-terminal configuration can be easily fabricated, either in a vertical stacked structure, similar to MTJs, or in a lateral transistor-like configuration. The latter is particularly interesting, since such a setup is easy to implement on new materials and allows to use either a top or a back-gate to manipulate spin currents using the Rashba effect (see Section 1.2). On the other hand, the simple structure leaves many boundary conditions, which have to be evaluated.

The two FM contacts create localized spin accumulations at their interface when applying an electric current, which move mainly through the electromagnetic potential of the applied electric field. An in-plane magnetic field can switch the FMs at their intrinsic coercive fields. This results in a difference of the resistance between the parallel and the anti-parallel

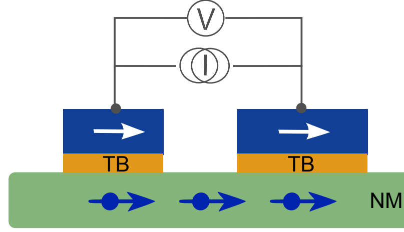

Figure 1.4: Local magnetoresistance measurement configuration. Spins are injected from a FM through a TB and can be detected by a second FM contact within the spin diffusion length of the material. The spin and charge transport are both driven by the applied electric field.

magnetization configuration of the FMs, which is detected as a step in a so called *spin valve* measurement (see Figure 1.5). Depending on the geometry additional boundary effects have to be considered: 1) For a lateral structure with an open or even infinite channel on either side of the electrodes (such as in Figure 1.4), the spins can diffuse away from the contacts against the electric field. 2) For a lateral structure confined between the two contacts (identical to a vertical structure), diffusion loses can be neglected. For the following discussion we assume the latter case, whereas the former can be derived similarly and just differs by a correction factor [35, 38].

The combined spin and charge current in the NM results in a solution for Equation (1.12) with non-zero values for the linear prefactors and both exponential terms due to the spin potential contribution by both FM contacts [38]. Taking the conservation of current into account, the magnetization alignment dependent resistances can be derived (see Equations (41) and (42) in [38]). Defining the resistance change between parallel (R_p) and anti-parallel (R_{ap}) magnetization orientation as $\Delta R = R_{ap} - R_p$, it can be fully expressed by

$$\Delta R = \frac{2\left(\beta R_{FM} + \gamma R_B\right)^2}{\left(R_B + R_{FM}\right)\cosh\left(\frac{t_{NM}}{\lambda_{NM}}\right) + \frac{R_{NM}}{2}\left[1 + \left(\frac{R_B}{R_{NM}}\right)^2\right]\sinh\left(\frac{t_{NM}}{\lambda_{NM}}\right)}. \tag{1.16}$$

Equation (1.16) requires the bulk polarization β and resistance R_{FM} of the FM, the interface polarization γ and resistance R_B of the insulating barrier, as well as the thickness t_{NM} and spin diffusion length λ_{NM} of the NM. The resistance for a parallel magnetization orientation is

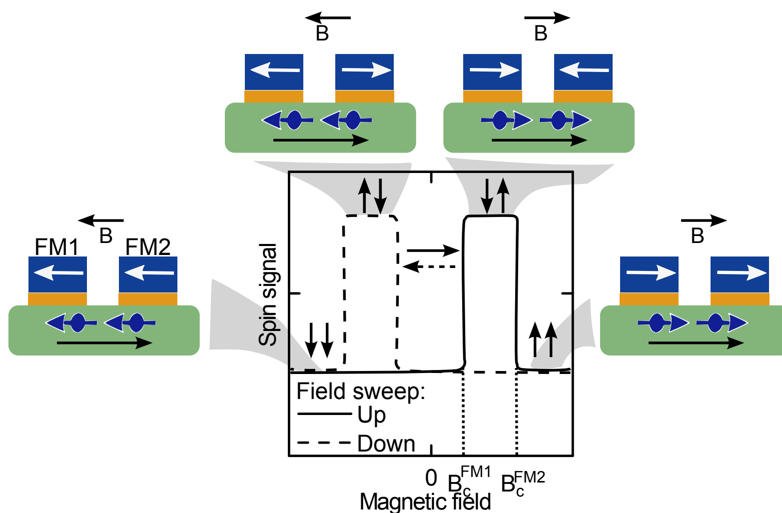

Figure 1.5: Spin signal line shape for a spin valve measurement. An applied in-plane magnetic field is swept from a negative to positive field (up sweep) and back to a negative field (down sweep). Meanwhile, it switches the magnetization directions of FM1 and FM2 at their coercive fields B_c^{FM1} and B_c^{FM2}, respectively. The spin signal reflects the detected magnetoresistance between a parallel and anti-parallel magnetization alignment.

$$R_{\uparrow\uparrow} = 2\left(1-\beta^2\right)R_{FM} + R_{NM}\frac{t_{NM}}{\lambda_{NM}} + 2\left(1-\gamma^2\right)R_B + 2\frac{\left(\beta-\gamma\right)^2 R_{FM}R_B + R_{NM}\left(\beta^2 R_{FM}+\gamma^2 R_B\right)\tanh\left(\frac{t_{NM}}{2\lambda_{NM}}\right)}{R_{FM}+R_B+R_{NM}\tanh\left(\frac{t_{NM}}{2\lambda_{NM}}\right)}. \tag{1.17}$$

The *magnetoresistance* (MR) is then defined as

$$MR = \frac{\Delta R}{R_{\uparrow\uparrow}}. \tag{1.18}$$

This result is very general and discussed for several structures in [35]. In the case of a FM/NM/FM structure without barrier resistance, thin and low resistive NM, Equation (1.18) becomes similar to Equation (1.4). Since MTJs usually have NM with varying resistances, it illustrates immediately

why it strongly depends on the interface layer and not only on the employed FM (as mentioned in Section 1.1).

A more realistic case is the FM/I/NM/I/FM structure with a barrier *interface* (I) between the FM and the NM. If we assume a SC NM, its resistance is usually much larger than the FM ($R_{NM} \gg R_{FM}$). That results in a confined range for the barrier resistance R_B to observe a significant MR:

$$R_{NM}\frac{t_{NM}}{\lambda_{NM}} \ll R_B \ll R_{NM}\frac{\lambda_{NM}}{t_{NM}}. \tag{1.19}$$

Physically this is easy to be understood: On one hand, if the barrier resistance is too small, the discontinuity in the chemical spin potential (see Section 1.3) introduced by the barrier is too small to create a significant spin accumulation. On the other hand, the finite spin lifetime limits the spin potential splitting, whereas the absolute potential increases with barrier resistance. This results in a drop of the MR if the barrier resistance becomes too large. Therefore, the barrier resistance needs to be optimized to achieve a high and detectable spin accumulation. Equation (1.18) is an excellent tool to predict this required resistance for contacts on novel materials.

It has to be mentioned that the combined spin and charge currents in the two-terminal structure can cause several effects which distort or affect the spin signal. Stray fields on the edges of the FM and external magnetic fields affect the current causing Hall effects, anisotropic MR [14], interference effects [44], and magneto-coulomb effects [45]. Even though this setup is highly interesting for applications, basic research tries to avoid these effects by using a *non-local* (NL) configuration.

1.4.2 Non-local spin transport measurement

In a NL measurement a spin accumulation is created in one circuit and detected in a separate pair of contacts (Figure 1.6). Spin and charge current are separated and the spins are transported from the injection contact to the detection contact by diffusion. Defining the position of the injector as $x = 0$, Equation (1.12) can be solved as

$$\mu_{\uparrow\downarrow} = \pm\mu_0 \cdot \exp\left(-\frac{x}{\lambda_{NM}}\right) \text{ for } x \geqq 0. \tag{1.20}$$

The individual spin currents through the interface can be written as

$$I_{\uparrow\downarrow} = \frac{I}{2} \pm \frac{\mu_0 \sigma_{NM} A}{e\lambda_{NM}}, \tag{1.21}$$

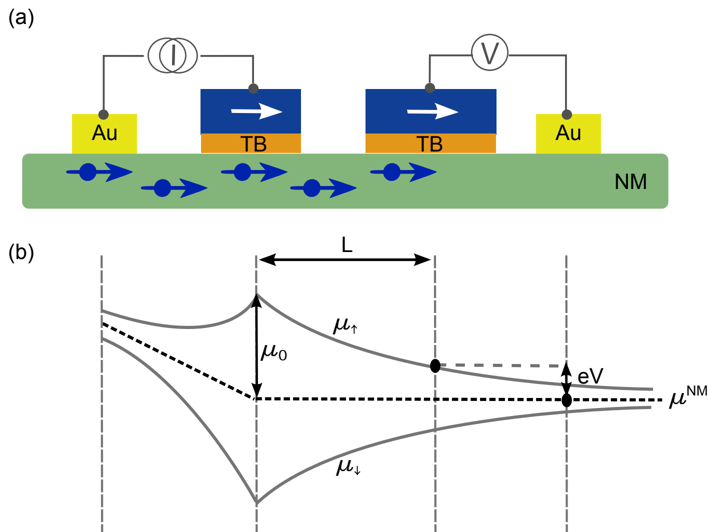

Figure 1.6: Non-local spin transport measurement configuration. (a) Schematic setup: spins are injected from a FM through a TB in the left circuit and can be detected in a similar circuit on the right. The spin transport in the non-magnetic material (NM) is diffusive. (b) The electrochemical potentials for up- and down-spins in the NM. The diffusing spins create a finite potential difference between either kind of spin potential, probed by the FM, and the equilibrium potential, probed by the Au contact.

where A is the cross section of the contact and I is the total tunnel current. The potential splitting at the interface ($x = 0$) can now be written as

$$2\mu_0 = e\left(V_\uparrow - V_\downarrow\right) = e\left(I_\uparrow R_\uparrow^{TB} - I_\downarrow R_\downarrow^{TB}\right) = \frac{eIR_{NM}\gamma_i}{1 + 2\frac{R_{NM}}{\left(R_\uparrow^{TB}+R_\downarrow^{TB}\right)}}, \qquad (1.22)$$

where γ_i is the injecting FM/I/NM interface spin polarization and the NM resistance is defined as

$$R_{NM} = \frac{\lambda_{NM}}{\sigma_{NM}A} = R_\square \frac{\lambda_{NM}}{W}, \qquad (1.23)$$

with the square resistance $R_\square$ and width W of the NM channel. If the ratio $\frac{R_{NM}}{\left(R_\uparrow^{TB}+R_\downarrow^{TB}\right)} = \frac{R_{NM}}{R_{TB}}$ in Equation (1.22) is large, then the spin potential splitting is reduced, identical as in the two-terminal model (Section 1.4.1). If the tunnel resistance is much larger than the NM resistance, the Equation (1.22) is simplified to

$$2\mu_0 = \mu_\uparrow - \mu_\downarrow = eIR_{NM}\gamma_i \qquad (1.24)$$

at the injector electrode.

The electrochemical potential is detected by a FM contact at a position $x = L$ defined by the sample geometry. Assuming that no net charge current flows through the detector, the detected potential is

$$\mu_{FM}(L) = \frac{\gamma_d [\mu_\uparrow(L) - \mu_\downarrow(L)]}{2} + \frac{\mu_\uparrow + \mu_\downarrow}{2}. \quad (1.25)$$

In contrast, a NM reference contact detects $\mu_{NM} = \frac{1}{2}[\mu_\uparrow + \mu_\downarrow]$ independent of its placement, since it exhibits no spin polarization. With Equation (1.20), (1.23), (1.24) and (1.25) one can calculate the NL voltage as:

$$V_{NL} = \frac{\mu_{FM} - \mu_{NM}}{e} = \pm\frac{\gamma_i \gamma_d R_\square \lambda_{NM}}{2W} \exp\left(-\frac{L}{\lambda_{NM}}\right). \quad (1.26)$$

This voltage can be measured by the detector in reference to a NM contact, or in reference to a FM contact at an infinite distance (see detector circuit in Figure 1.6). The signal is positive if the magnetization of the detector and injector are parallel, and vice versa. This is similar to the *spin valve signal* presented in Figure 1.5 of Section 1.4.1, except that the spin current is driven diffusively between injector and detector electrode. It is measured by sweeping a magnetic field $B_{||}$ in-plane and magnetization direction. By fabricating the injector and detector accordingly, different switching fields are achieved (Section A.3.3.3). This allows to distinct between both magnetization orientations in one magnetic sweep where a step of $2V_{NL}$ can be observed (see Figure 1.5). This step equals the voltage difference between the parallel and anti-parallel configuration during the field sweep.

Non-local Hanle measurement

The Hanle effect can be used to control the dephasing of the spins by an external magnetic field. This is detected as a reduction of the voltage signal in Equation (1.26). In contrast to the NL spin valve signal, a magnetic field $B_\perp$ is applied perpendicular to the magnetization, hence also to the spin polarization direction. This causes the spins to precess with the Larmor frequency

$$\omega_\mathrm{L} = \frac{g\mu_B B_\perp}{\hbar}. \quad (1.27)$$

The precession yields to a dephasing of the spins and consequently the polarization is lost. This effect was first observed by Wood and Ellett in 1923, and described by Hanle in 1924 [46]. For ballistic transport the spin